Cement and Concrete Research 40 (2010) 1314–1319

Contents lists available at ScienceDirect

Cement and Concrete Research

journal homepage: http://ees.elsevier.com/CEMCON/default.asp

Characterisation of iron inclusion during the formation of calcium sulfoaluminate phase

M. Idrissi [a,*], A. Diouri [a], D. Damidot [b], J.M. Greneche [c], M. Alami Talbi [a], M. Taibi [d]

[a] Laboratoire de Chimie du Solide Appliquée, Faculté des Sciences, B.P. 1014. R.P. — Avenue Ibn Battouta, 10000 Rabat, Morocco
[b] Département de Génie Civil et Environnemental, Ecole des Mines de Douai, 941 Rue Charles Bourseul, 59500 Douai, France
[c] Laboratoire de Physique de L'Etat Condensé, UMR CNRS 6087 Institut de Recherche en Ingénierie Moléculaire et Matériaux Fonctionnels IRIM2F, FR CNRS 2575, Université du Maine, France
[d] Laboratoire de Physico-chimie des Matériaux, Ecole Normale Supérieure, Rabat, Morocco

ARTICLE INFO

Article history:
Received 13 May 2009
Accepted 15 February 2010

Keywords:
Thermal treatment (A)
EDX (B)
Microstructure (B)
X-ray diffraction (B)
$3CaO \cdot 3Al_2O_3 \cdot CaSO_4$ (D)

ABSTRACT

The iron distribution among the sulfoaluminate clinker phases and its ability to enter the calcium sulfoaluminate lattice in solid solution can have a significant influence on manufacturing process and reactivity of calcium sulfoaluminate (CSA) cements. X-ray diffraction (XRD) analysis, Mössbauer spectroscopy, scanning electron microscopy (SEM) equipped with an energy dispersive X-ray analysis system (EDAX) and infrared spectroscopy were used to identify the mineralogical conditions of iron inclusion during the formation of calcium sulfoaluminate (C_4A_3S) phase from different mixtures in the $CaO–Al_2O_3–Fe_2O_3–SO_3$ system. The mixtures, heated in a laboratory electric oven, contained stoichiometric amounts of reagent grade $CaCO_3$, Al_2O_3, Fe_2O_3 and $CaSO_4 \cdot 2H_2O$ for the synthesis of $Ca_4Al_{(6-2x)}Fe_{2x}SO_{16}$, where x, comprised between 0 and 3, is the mole number of Al_2O_3 substituted by Fe_2O_3. With x increasing from 0 to 1.5, both the iron content of C_4A_3S phase and the amounts of side components such as C_2F and CS increased. For x values included in the range of 1.5–3.0, at temperatures higher than 1200 °C, melting phenomena were observed and, instead of the C_4A_3S solid solution, ferritic phases and anhydrite were formed.

1. Introduction

The mineral phase, calcium sulfoaluminate $Ca_4Al_6SO_{16}$ also named yeelimite and written C_4A_3S in cement notation, is known as a hydraulic phase. It may be the major component of new cements having a lower environmental impact. Indeed sulfoaluminate cement (SAC) and ferroaluminate cement (FAC) contain more than 30 percent of calcium sulfoaluminate along with belite (C_2S) and calcium ferrite [1,2]. Much research has been devoted to optimize the clinkering conditions using different raw materials or by-products [3–6]. The sintering temperature of this type of cement is in the range of 1200–1350 °C. The CO_2 emissions are lower compared to those of ordinary Portland cement heated at 1400–1450 °C. It is therefore of great importance to know the thermal stability of the mineralogical phases contained in sulfoaluminate and ferroaluminate cements to understand the effect of inclusion of certain chemical elements on the stability and hydraulic reactivity of these phases. According to the literature, the effect of minor components on the formation of clinker varies. It depends on its function and its ability to act as flux and/or mineralizing. These components can reduce the formation temperature of the liquid phase and/or increase the quantity melted, accelerating the rate of reaction occurring in solid, or liquid–solid interface and affect both crystal growth and morphology.

The technological consequences are evident; they involve changes in the reactivity and burnability of the raw materials, formation of new phases in altered amounts, differentiation of hydraulic activity and properties of produced cements.

Generally calcium sulfoaluminate cements are produced from raw materials such as bauxite, red mud, limestone and gypsum [7]. Essentially, the bauxite and red mud can present high proportions of iron which influence the mineralogy and reactivity of clinker phases. Indeed Fe_2O_3 content in these materials can vary from 1 to 33 wt.% against 0.5 to 6% in OPC materials [8]. Thus the knowledge of the conditions of iron inclusion in $Ca_4Al_6SO_{16}$ phase, its maximum content and its impact on reactivity can constitute a primordial factor in the manufacturing process. It was firstly reported by Halstead et al. [9] that the maximum iron insertion depends on the crystal structure of C_4A_3S. The structure was described in cubic sub crystalline cell ($a = 9.195$ Å). The space group $I\bar{4}3m$ is after determined by H. Sealfeld et al. [10]. By the salt-fusing synthesized method of monocrystal, F. Xiuji et al. [11] pointed the space group in $I4_132$ and determined the atom coordinates. The refinement of the parameters was conducted by Z. Peixing et al. [12], the structure was indexed in tetragonal system $P\bar{4}C2$, with lattice parameters $a = b = 13.031$ Å and $c = 9.163$ Å. Another investigation was conducted by Ikeda et al. and shows that C_4A_3S is indexed in cubic cell but with lattice parameter $a = 18.42$ Å in I23 space group [13]. However, the neutron powder diffraction data of this phase were also refined by the Rietveld profile technique [14], the orthorhombic space group Pcc2 is determined with cell parameters $a = 13.028$ Å, $b = 13.037$ Å, and $c = 9.161$ Å. According to the research reported by Teoreanu et al. [15],

* Corresponding author. Tel.: +212 668831247; fax: +212 5 37 77 42 61.
E-mail address: mari_idrissi@yahoo.fr (M. Idrissi).

0008-8846/$ – see front matter © 2010 Elsevier Ltd. All rights reserved.
doi:10.1016/j.cemconres.2010.02.009

Table 1
Chemical compositions (wt.%) of starting mixtures in samples S00–S30.

Sample	%$CaCO_3$	%$CaSO_4 \cdot 2H_2O$	%Al_2O_3	%Fe_2O_3
S00	38.58	22.12	39.3	–
S01	38.3	21.96	37.71	2.04
S02	38.02	21.8	36.14	4.04
S04	37.47	21.48	33.08	7.97
S05	37.2	21.33	31.58	9.89
S08	36.42	20.88	27.21	15.49
S10	35.92	20.59	24.39	19.1
S15	34.72	19.91	17.68	27.69
S30	31.56	18.09	–	50.35

these authors claimed to have found some compounds having the general formulae of $3CaO–Al_2O_3–M_x(SO_4)_y$ ($M = Mg^{2+}$, Sr^{2+},Ba^{2+}, Fe^{3+}, $A1^{3+}$). Chen et al. [16] have determined that a maximum of iron solid solution in the $3CaO–3Al_2O_3–CaSO_4$ system is reached at 22.61 wt.% of Fe_2O_3. On the other hand, Huang et al. [17] have tested the influence of Fe_2O_3 on the formation of C_4A_3S by X-ray diffraction and concluded that the maximum quantity of the phase can be obtained at 1300 °C in specimens doped with 1% Fe_2O_3 and that half-hour of thermal treatment time is delayed with 3% and 5% Fe_2O_3 at 1350 °C. Feng and Long [18] studied the effects of phosphate, fluorite, ferrite and titanium oxides on the formation and properties of $3CaO–3Al_2O_3–CaSO_4$ in sulfoaluminate cement. Other minor oxides (TiO_2, ZnO, and Cr_2O_3) and burning temperature's effect on the formation and decomposition of $3CaO–3Al_2O_3–CaSO_4$ were investigated by Y. Li et al. [19]. These results show that Fe_2O_3 and CaF_2 promote the formation of $3CaO–3Al_2O_3–CaSO_4$ and $CaSO_4$ decomposition while maintaining the rate adopted TiO_2, ZnO and Cr_2O_3 in the formation of $3CaO–3Al_2O_3–CaSO_4$ because of their stabilizing effect. The addition of Cr_2O_3 and Fe_2O_3 decreases the decomposition temperature of $3CaO–3Al_2O_3–CaSO_4$, Benarchid et al. [20] studied the influence of elements Cr and P on the formation of calcium sulfoaluminate, and they concluded that this phase is stable at high concentration of these additives. Although it could have been interesting to investigate the competition between aluminium and iron oxides for both the calcium sulfoaluminate generation and the synthesis of minor clinker components, this work was devoted to study the C_4A_3S formation from stoichiometric mixtures of reagent grade $CaCO_3$, Al_2O_3, Fe_2O_3 and $CaSO_4 \cdot 2H_2O$. The mixtures were heated in a laboratory electric oven for obtaining $Ca_4Al_{(6-2x)}Fe_{2x}SO_{16}$, where x, comprised between 0 and 3, is the mole number of Al_2O_3 substituted by Fe_2O_3. The results of characterization techniques such as X-ray diffraction (XRD) analysis, Mössbauer spectroscopy, scanning electron microscopy (SEM) equipped with an energy dispersive X-ray analysis system (EDAX) and infrared spectroscopy were correlated in order to identify the mineralogical conditions of iron inclusion during the formation of the C_4A_3S solid solutions.

2. Preparation and methods

2.1. Samples preparation

The samples were synthesized from stoichiometric amounts of reagent grade $CaCO_3$, Al_2O_3, Fe_2O_3 and $CaSO_4 \cdot 2H_2O$ with >99% purity. Batches of 20 g were ground in an agate mortar with ethanol as dispersive and homogeneity medium. The burning of the samples were carried out in platinum crucible in a laboratory furnace at different temperatures at 500 °C, 800 °C, 1000 °C, and 1100 °C, with an intermediate grinding in order to increase the homogeneity. The final clinker was yet heated directly at final temperature: 1200, 1250, 1300 or 1350 °C, as a function of the considered case. The adopted formula is $Ca_4Al_{(6-2x)}Fe_{2x}SO_{16}$ in which x is the mole number of Al_2O_3 substituted by Fe_2O_3. The mixtures have been synthesized for $0 \leq x \leq 3$ and were named from S00 to S30. The corresponding chemical compositions (weight percent oxide) are reported in Table 1. For rich iron compositions, beyond $x = 1.5$, we observe an early melting of samples at treatment temperatures above 1200 °C. The investigations and the interpretation of the results will focused essentially on the samples located in the interval (0–27.69 wt.% of Fe_2O_3) which corresponds to $0 \leq x \leq 1.5$. Beyond this interval, the amount of iron is too high and the analysis by X-ray diffraction shows mainly the formation of $Ca_2Fe_2O_5$ phase and anhydrite.

2.2. Methods of investigation

2.2.1. X-ray diffraction

The mineralogical analysis was made by X-ray diffraction using a D8 Advance diffractometer (Bruker) with Co K_α radiation (1.7889 Å). Specimens were step-scanned as random powder mounts from 5 to 100° 2θ

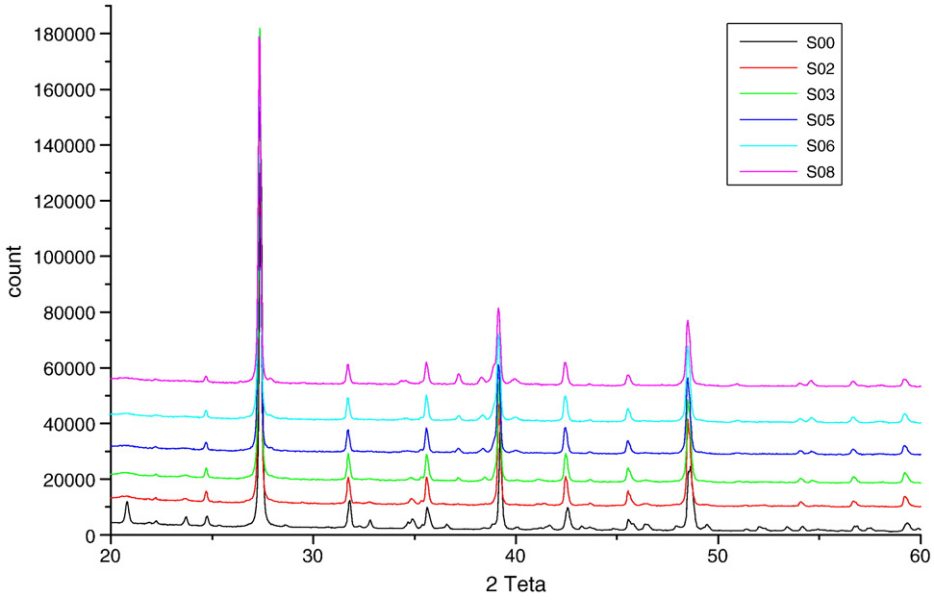

Fig. 1. XRD patterns of pure and doped calcium sulfoaluminate. Samples: S00 heated at 1350 °C and S02–S08 heated at 1250 °C.

Table 2
Semi-quantitative XRD identification of mineralogical phases in the samples S00–S30 heated at 1250 °C. +++: high quantity, ++: average quantity, +: little quantity, −: trace.

	S00	S01	S02	S04	S05	S10	S15	S30
C_4A_3S	+++	+++	+++	+++	+++	+++	++	
CS	+	+					++	++
C_2F			−	+	+	+	++	+++

at 0.036° 2θ steps integrated at 30 s step^{-1}. To compare the obtained results, we have used tetragonal phase C_4A_3S (ASTM 01-85-2210) as reference.

2.2.2. ^{57}Fe Mössbauer spectrometry

The Mössbauer spectra were collected at 300 K in transmission mode using a conventional constant-acceleration spectrometer and a ^{57}Co source in Rh matrix. The absorbers were obtained by pressing the powdered sample into Holder acceleration; the velocity scale was calibrated using α-Fe foil while the isomer shift values are quoted relative to α-Fe at 300 K.

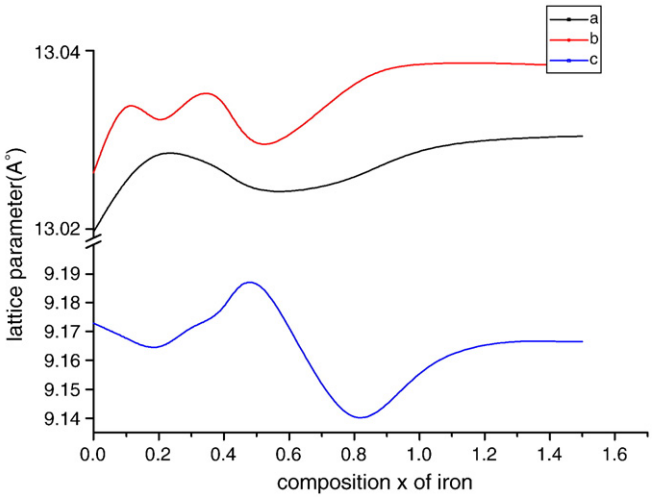

Fig. 2. Variation of lattice parameters *a*, *b* and *c* of doped C_4A_3S, indexed in Pcc2 orthorhombic space group, as a function of iron inclusion.

2.2.3. Scanning electron microscopy

The scanning electron micrographs were obtained on polished sections in backscattered mode using the HITACHI S-4300 SE/N. The acceleration voltage was 20 kV. EDAX was used for the chemical analysis Noram (system six).

2.2.4. IR-Spectroscopy

Infrared spectroscopy was carried out on some selected samples to provide additional information on the samples. One milligram of the powder sample was ground with 100 mg of KBr in agate mortar to produce a homogeneous mixture and then pressed to transparent discs with a diameter of 1 cm. The infrared spectral analysis was recorded from KBr-discs using PerkinElmer FT-IR RXI spectrometer in the range of 400–1300 cm^{-1}.

3. Results and discussion

3.1. Mineralogical characterization

The evolution of mineralogical composition at 1100 °C shows the formation of calcium sulfoaluminate phase with a small quantity of CA phase and anhydrite $CaSO_4$. A decrease of the CA and $CaSO_4$ amounts depends on the increase of the concentration of Fe_2O_3 oxide and the treatment temperature. The identified crystalline phases, in burned clinkers at 1250 °C and their semi-quantitative estimate, by X-ray diffraction are given in Fig. 1 and Table 2. The compositions ranging between S02 and S10 are constituted by C_4A_3S which is accompanied by the formation of C_2F phase known as a solid solution that it is always formed, in the presence of both Al_2O_3 and Fe_2O_3, in the form of $Ca_2(Fe_{1-x}Al_x)_2O_5$, some reduction of Fe^{3+} to Fe^{2+} occurs when the ferrite phase is prepared in air, which is our experimental conditions, it leads to the formation of minor amounts of other phases which are not observed by X-ray diffraction [21–23].

At low percentage of iron (S01) or without iron (S00), CA and $CaSO_4$ are observed at 1250 °C but disappear at 1300 °C and 1350 °C, for S01 and S00 respectively. In similar conditions of treatment, Y. Huang et al. have also observed the presence of $CaSO_4$ at temperatures above 1250 °C and adjacent to 1350 °C [17], this may be due to the oxidizing conditions of air treatment and the presence of Al_2O_3 and Fe_2O_3 [24].

From XRD patterns, all of the peaks corresponding to C_4A_3S are indexed in orthorhombic cell with space group Pcc2 which is in good

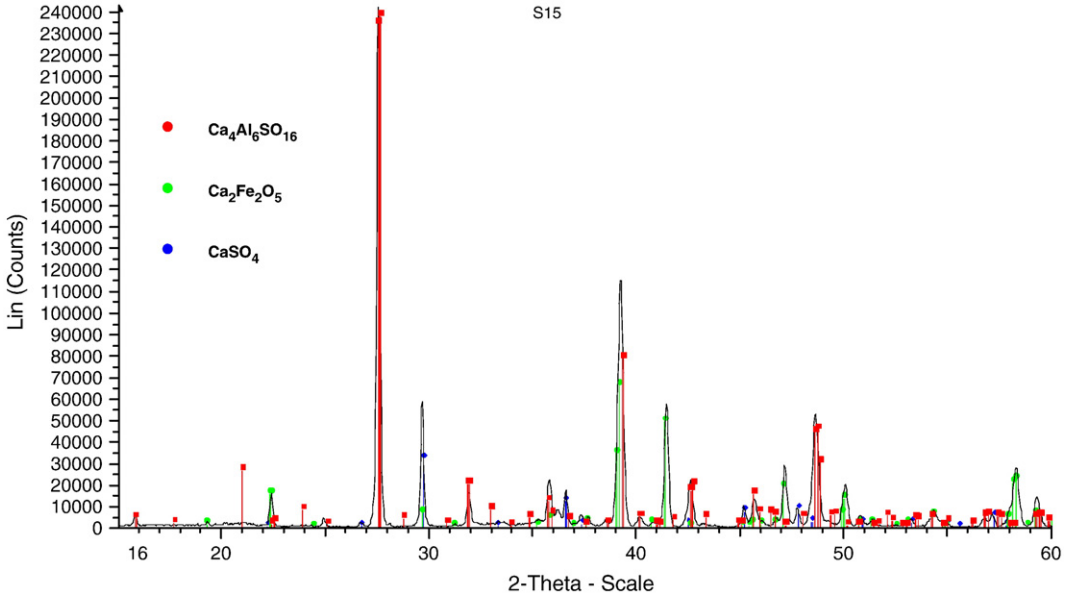

Fig. 3. XRD pattern of iron doped calcium sulfoaluminate sample S15 heated at 1250 °C.

agreement with the results of Nickolas et al. [14]. In our samples, the calculated cell parameters show a slight anisotropy (12.99 Å ≤ *a* ≤ 13.03 Å, 12.99 Å ≤ *b* ≤ 13.05 Å, and 9.14 Å ≤ *c* ≤ 9.20 Å) which explains the flexibility of the cell. As regard the results of Osokin et al. [8] and Chen et al. [16], those authors have determined the parameters of the lattice from a cubic system and observed a linear variation up to the limit of solid solution. Our results show changes in parameters of the lattice indexed in orthorhombic system, when the two parameters *a* and *b* vary in a same sense, the third parameter *c* varies in the opposite direction and vice-versa (Fig. 2). From composition S02 to higher iron contents, the presence of peaks corresponding to C_2F can be explained by the fact that not all of the added iron is included in the lattice of calcium sulfoaluminate. The presence of C_4A_3S which is mixed with C_2F, is also observed with CS for sample S10 and those having greater iron contents (Fig. 3).

3.2. ^{57}Fe Mössbauer spectrometry

A preliminary study using Mössbauer spectrometry permitted to analyse some samples (S02, S04, S08, and S15) heated at 1250 °C and S30 at 1200 °C (Fig. 4). We have analysed the sample S30 (in absence of alumina oxide) of which the XRD spectra consisted of C_2F and $CaSO_4$ phases. The Mössbauer spectrum of this sample indicated the presence of a preponderant doublet representing the paramagnetic repartition of iron element in C_2F phase. In sample S02, in addition to the similar doublet of C_2F, a low sextuplet reflecting another type of Fe was observed. It is probably due to a low inclusion of iron in the sulfoaluminate phase. In other samples, S04, S08 and S15, the phenomenon is growing and the presence of two types of hyperfine sextuplets corresponding to Fe^{3+} in tetrahedral and octahedral environments was clearly observed. These two sextuplets are likely to be related to calcium sulfoaluminate doped with iron. In S15 sample, a third sextuplet is observed. The reduction of the hyperfine fields at ^{57}Fe sites compared to those of $Ca_2Fe_2O_5$ are due to the presence of diamagnetic Al cations as first neighbour and to the effects of chemical and structural disorder in the form $Ca_2(Fe_{1-x}Al_x)_2O_5$ of C_2F [25–27].

In sum, this technique allowed us to identify different forms of iron when it is in C_2F phase alone and when it is simultaneously included in yeelimite phase as $Ca_4Al_{(6-2x)}$ $Fe_{2x}SO_{16}$ form and in C_2F phase as $Ca_2(Fe_{1-x}Al_x)_2O_5$ form.

3.3. Scanning electron microscopy

The micrographs corresponding respectively to S00, S02, S05, S08, S15 and S30 samples are represented in Fig. 5. For the single phase C_4A_3S (S00), the crystals are homogeneous having a dark grey colour. The samples S02–S08 show large proportions of $C_4(A, F)_3S$ and the formation of little quantities of C_2F phase (having a lighter grey level). The quantities of C_2F increase from S02 to S08. Samples S15–S30 show the emergence of unreacted $CaSO_4$ in the presence of large quantities of C_2F. EDAX analysis gave the percentage of different elements analysed in the C_4A_3S phase doped with iron. The average of different atomic percent calculated from several analysed points (more than ten points for each sample) of C_4A_3S area is reported in Table 3. The electronic balance of the formulae in this table shows that the C_4A_3S phase is in the form of a lacunar solid solution which explains the observed deficiencies in calcium.

We observe that the inclusion of Fe in the sulfoaluminate phase increases according to the proportions of iron in the formula, in despite of the increasing amount of the ferritic phase. The deficiency amount of calcium in $C_4(A, F)_3S$ phase maybe interpreted like to the probably substitution of iron also to calcium. This result can explain the presence of the two types of hyperfine sextets due to Fe^{3+}, observed by Mössbauer measurements in the same samples.

3.4. Infrared spectroscopy

The infrared absorption spectra of S00, S02, S08, S20 and S30 showed the vibration frequencies of different groups of pure and doped C_4A_3S in the range of 400–1300 cm^{-1} (Fig. 6). $[AlO_4]$ groups are identified at 411, 644, 690, 821 and 875 cm^{-1}. Absorption bands located at 615, 663, 987, 1100, 1149 and 1195 cm^{-1} are assigned to the $[SO_4]$ groups [28,29]. A diminution of the $[AlO_4]$ groups is observed by adding iron and it disappears in sample S30. The data show also a shift

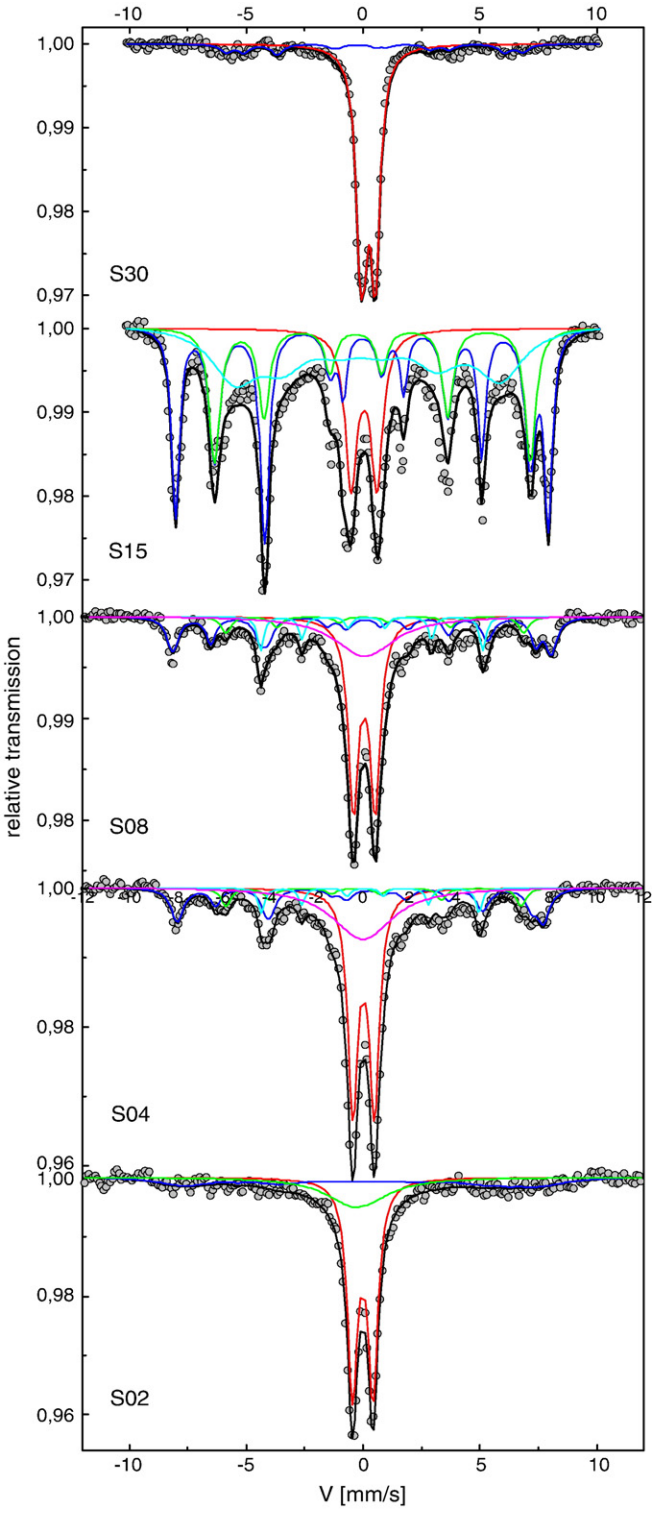

Fig. 4. Mössbauer spectra of S02, S04, S08, S15 and S30 samples at $T = 300$ K.

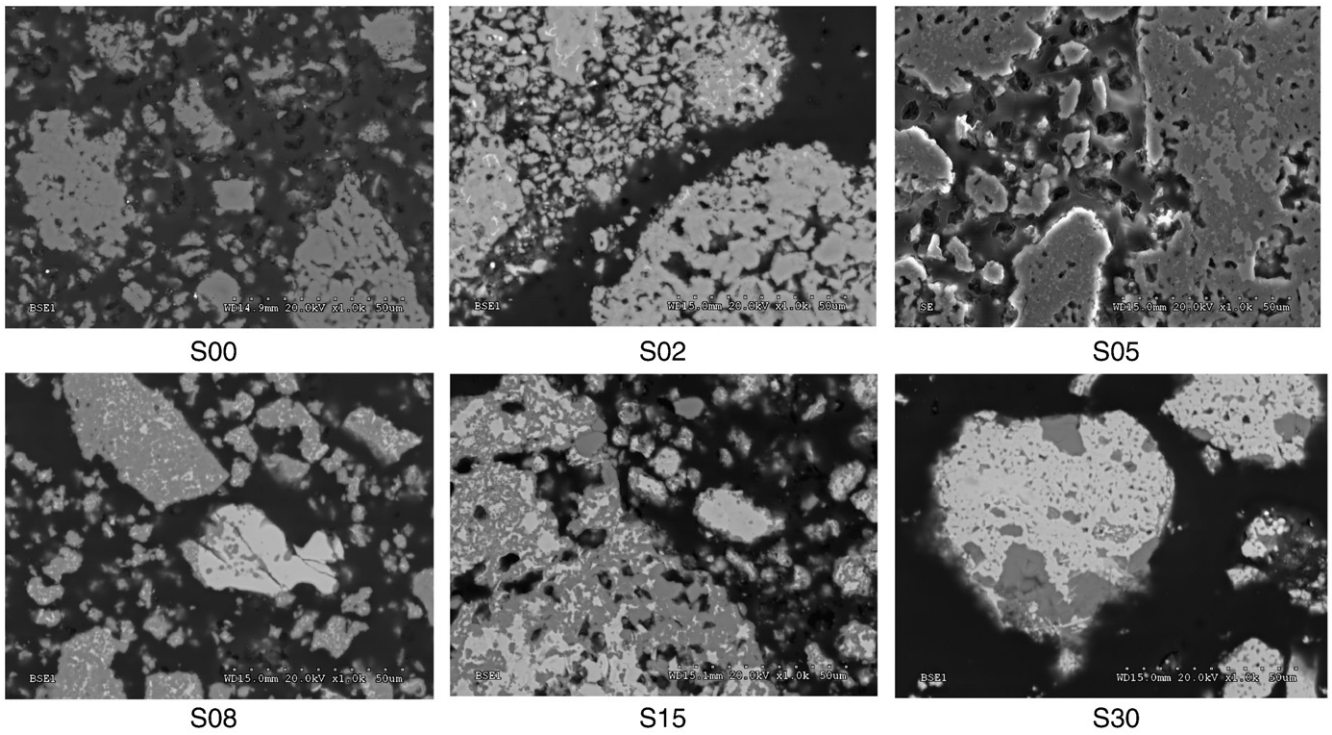

Fig. 5. Scanning electron micrographs of pure and iron doped calcium sulfoaluminate phase.

Table 3
Average formula of at.% in C_4A_3S area of samples S00–S15 analysed by EDAX.

Samples	Theoretical formula	Average analysed formula	(wt.%) Fe in C_4A_3S phase	(wt.%) Fe_2O_3 in starting mixtures
S00	$Ca_4Al_6SO_{16}$	$Ca_{3.59}Al_{5.34}S_{0.77}O_{15.3}$	0	0
S02	$Ca_4Al_{5.6}Fe_{0.4}SO_{16}$	$Ca_{3.76}Al_{4.79}Fe_{0.35}S_{1.05}O_{15.05}$	3.41	4.04
S05	$Ca_4Al_5Fe_1SO_{16}$	$Ca_{3.79}Al_{4.48}Fe_{0.89}S_{0.89}O_{14.94}$	8.42	9.89
S08	$Ca_4Al_{4.4}Fe_{1.6}SO_{16}$	$Ca_{3.98}Al_{4.33}Fe_{1.33}S_{0.83}O_{14.73}$	12.12	15.49
S15	$Ca_4Al_3Fe_3SO_{16}$	$Ca_{3.82}Al_{3.48}Fe_{2.47}S_{0.77}O_{14.47}$	21.51	27.69

and the spreading of the band referring to the various oscillations of the SO_4^{2-} group in the original C_4A_3S (absorption bands 1099 and 1192 cm^{-1}). This is due to a change in the coordination environment of that group as a result of the incorporation of ferrite oxide according to Osoking et al. [8].

4. Conclusion

A considerably different behaviour was shown by stoichiometric mixtures of reagent grade $CaCO_3$, Al_2O_3, Fe_2O_3 and $CaSO_4 \cdot 2H_2O$, conceived for obtaining, upon heating in a laboratory furnace, a calcium sulfoaluminate phase corresponding to the formula $Ca_4Al_{(6-2x)}Fe_{2x}SO_{16}$ in which x ranges from 0 to 3 and represents the mole number of Al_2O_3 substituted by Fe_2O_3. For x values comprised between 1.5 and 3.0, at temperatures higher than 1200 °C, an early melting occurred and the formation of ferritic phases and anhydrite was observed. For x values included in the range of 0–1.5, calcium sulfoaluminate was the main

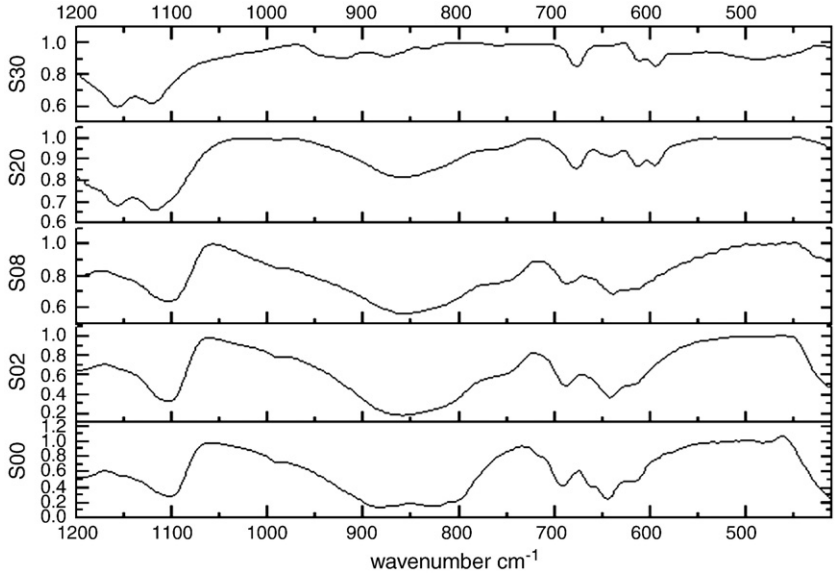

Fig. 6. Infrared spectra of samples S00–S30.

phase. With the increase of x, the iron content introduced in the C_4A_3S lattice increased, but the selectivity of the reacting system towards the calcium sulfoaluminate phase decreased, and the presence of dicalcium ferrite and anhydrite was detected. All the calcium sulfoaluminate preparations had a deficiency of calcium and showed small variations in the values of the cell parameters. Under the experienced conditions, the maximum iron concentration in the calcium sulfoaluminate phase was 21.5 wt.%.

Acknowledgement

The authors would like to thank EGIDE for the financial support given by the grant No. MA/05/119F in the framework of a France–Morocco exchange program.

References

[1] Tangbo Sui, Yan Yao, Recent progress in special cements in China, Proc. 11th Int. Congr.Chem. Cem., Durban, South Africa, 4, 2003, pp. 2028–2032.
[2] Ellis Gartner, Industrially interesting approaches to low-CO2 cements, Cement and Concrete Research 34 (2004) 1489–1498.
[3] Graziella Bernardo, Milena Marroccoli, Fabio Montagnaro, Gian Lorenzo Valenti, Use of Fluidized Bed Combustion Wastes for the Synthesis of Low Energy Cements, ICCC, Durban, 2003, pp. 1227–1236.
[4] M. Katsioti, P.E. Tsakiridis, T.S. Agatzini-Leonardou, P. Oustadakis, Examination of the jarosite–alunite precipitate addition in the raw meal for the production of Portland and sulfoaluminate-based cement clinkers, International Journal of Mineral Processing 76 (2005) 217–224.
[5] P. Arjunan, Michael R. Silsbee, Della M. Roy, Sulfoaluminate–belite cement from low-calcium fly ash and sulfur-rich and other industrial by-products, Cement and Concrete Research 29 (1999) 1305–1311.
[6] C.A. Luz, J.C. Rocha, M. Cheriaf, J. Pera, Valorization of galvanic sludge in sulfoaluminate cement, Construction and Building Materials 23 (2009) 595–601.
[7] N. Fukuda, Short Communications 34 (1961) 138–139.
[8] A.P. Osokin, Y.R. Krivoborodov, S.V. Samchenko, Expansive and Non-Shrinkage Sulfoaluminate Cements, ICCC, Durban, 2003, pp. 2083–2087.
[9] P.E. Halstead, A.E. Moore, Journal of Applied Chemistry 12 (9) (1962) 413.
[10] H. Saalfeld and W. Depmeier, Kristall and Technik, (1972), 7, 229, 1–3.
[11] Feng Xiuji, Liao Guanglin, Journal of Wuhan University of Technology, (China) 1 (3) (1988).
[12] Z. Peixing, C. Yimin, S. Liping, Z. Guanying, H. Wenmei, W. Jianguo, The Crystal Structure of C_4A_3S, 9th ICCC, NewDelhi, 1992, pp. 201–208.
[13] K. Ikeda, K. Kishimoto, H. Shima, Structure refinement of calcium sulfoaluminate, with emphasis to oxygen deficiency, Cement and Concrete Research 26 (1996) 743–748.
[14] Nickolas J. Calos, Journal of Solid State Chemistry 119 (1995) 1–7.
[15] Teoreanu, M. Muntean and I. Dragnea, Cemento, Type $3(CaO\cdot Al_2O_3)$ $(M_x\cdot SO_4)_y$ compounds and compatibility relations in $CaO–CaO\cdot Al_2O_3–M_x(SO_4)_y$ systems. (1986), 83, 39–46.
[16] D. Chen, Xiuji Feng, Shizhong Long, The influence of ferric oxide on the properties of 3CaO·3Al2O3·CaSO4, Thermochimica Acta 215 (1993) 157–169.
[17] Huang Yeping, Shen Xiaodong, Ma. Suhua, Chen Lin, Zhong Baiqian, Effect of Fe_2O_3 on the formation of calcium sulfoaluminate mineral, Journal of the Chinese ceramic society 35 (2007).
[18] X.J. Feng, S.Z. Long, Proc. 2th Symp. On Cem. Chem. of China, Beijing, Building Industrial Press of China, 1988, pp. 339–344.
[19] Y. Li, X. Liu, X. Niu, L. Song, Materials Research Innovations (2007) 11.
[20] My.Y. Benarchid, J. Rogez, A. Diouri, A. Boukhari, J. Aride, Formation and hydraulic behavior of chromium–phosphorus doped calcium sulfoaluminate cement, Thermochimica Acta 433 (2005) 183–186.
[21] A.J. Majumdar, Transactions and Journal of the British Ceramic Society 64 (1965) 105.
[22] M. Maultzsch, H. Scholze, Formation of the ferritic clinker phases from the melt, Zement-Kalk-Gips 26 (1973) 583–587.
[23] H.F.W. Taylor, Cement Chemistry, Thomas Telford, London, UK, 1997, pp. 24–37.
[24] Naoto Mihara, Dalibor Kuchar, Yoshihiro Kojima, Hitoki Matsuda, Reduction decomposition of waste gypsum with SiO_2, Al_2O_3 and Fe_2O_3 additives, Journal Material Cycles and Waste Management 9 (2007) 21–26.
[25] K.S. Harchand, K. Chandra, A study of CaO $(Fe_2O_3)_{1-x}(Al_2O_3)_x$ system, Cement and Concrete Research 13 (4) (1983) 465–469.
[26] R. Kumar, Vishwamittar, K. Chandra, Low temperature Mössbauer spectroscopic study of $CaO(Fe_2O_3)_{1-x}(Al_2O_3)_x$ system, Cement and Concrete Research 15 (3) (1985) 520–524.
[27] B.S. Randhawa, Kamaljeet Sweety, Calcium ferrite formation from the thermolysis of calcium tris (maleato) ferrate(III), Bulletin of Material Science 23 (4) (2000) 305–307.
[28] X. Liu, Y. Li, N. Zhang, Influence of MgO on the formation of Ca_3SiO_5 and $3CaO\cdot 3Al_2O_3\cdot CaSO_4$ minerals in alite–sulphoaluminate cement, Cement and Concrete Research 32 (2002) 1125–1129.
[29] P. Zhang, Y. Chen, L. Shi, G. Zhang, W. Huang, J. Wu, Proceedings of the Ninth ICCC, New Delhi, India, 3, 1992, pp. 201–208.